Adipocyte Liver Kinase b1 Suppresses Beige Adipocyte Renaissance Through Class IIa Histone Deacetylase 4

Yangmeng Wang,[1,2] Esther Paulo,[1] Dongmei Wu,[1] Yixuan Wu,[1] Wendong Huang,[2] Ajay Chawla,[1] and Biao Wang[1]

Diabetes 2017;66:2952–2963 | https://doi.org/10.2337/db17-0296

Uncoupling protein 1$^+$ beige adipocytes are dynamically regulated by environment in rodents and humans; cold induces formation of beige adipocytes, whereas warm temperature and nutrient excess lead to their disappearance. Beige adipocytes can form through de novo adipogenesis; however, how "beiging" characteristics are maintained afterward is largely unknown. In this study, we show that beige adipocytes formed postnatally in subcutaneous inguinal white adipose tissue lost thermogenic gene expression and multilocular morphology at the adult stage, but cold restored their beiging characteristics, a phenomenon termed beige adipocyte renaissance. Ablation of these postnatal beige adipocytes inhibited cold-induced beige adipocyte formation in adult mice. Furthermore, we demonstrated that beige adipocyte renaissance was governed by liver kinase b1 and histone deacetylase 4 in white adipocytes. Although neither presence nor thermogenic function of uncoupling protein 1$^+$ beige adipocytes contributed to metabolic fitness in adipocyte liver kinase b1–deficient mice, our results reveal an unexpected role of white adipocytes in maintaining properties of preexisting beige adipocytes.

Energy balance requires equivalent energy intake and energy expenditure, and when energy intake exceeds energy expenditure, animals store excess energy as fat in adipose and other metabolic tissues. Chronic energy excess can lead to obesity and further development into type 2 diabetes (1). Adaptive thermogenesis, a major contributor of total energy expenditure, occurs mostly in brown fat (2), which contains specialized mitochondria-rich brown adipocytes for which thermogenic functionality is conferred by the uncoupling protein 1 (UCP1) (3,4). The presence of thermogenic UCP1$^+$ fat depots in adult humans has been recognized recently using ^{18}F-fluorodeoxyglucose positron emission tomography scan (5–7). In small rodents such as mice and rats, two types of UCP1$^+$ adipocytes have been distinguished by their localization and developmental origin. Classic, also called constitutive, brown adipocytes are present in interscapular and perirenal adipose tissues, and they originate from Myf5$^+$/Pax7$^+$ skeletal muscle progenitors (8). In contrast, Ucp1$^+$ multilocular adipocytes are also found scattered within white adipose tissue (WAT) in response to β-adrenergic (βAR) stimulation (9–13). These Ucp1$^+$ multilocular brown adipocytes in WAT are called beige adipocytes (or inducible brown adipocytes), although the multilocular morphology and Ucp1 expression are not always coupled (14,15). Notably, beige adipocytes in WAT are functionally identical as brown adipocytes in interscapular brown adipose tissue (iBAT) at the single-cell level. Indeed, the mitochondria from Ucp1$^+$ multilocular adipocytes in inguinal WAT (iWAT) and brown adipocytes in iBAT process similar thermogenic capacity in vitro (4).

The beige adipocyte formation is dominantly determined by the strength of βAR signaling in white adipose tissues, including amounts of catecholamines, βAR abundance, and its intracellular signaling on target cells. Various sources can release catecholamines to induce browning. Sympathetic activation by cold and hormones has been recognized to be a dominant driver of beige adipocyte recruitment in both rodents and humans (16). Myeloid cells can synthesize and secrete catecholamines to induce browning, especially under thermoneutral condition in mice (17). Moreover, excess

[1]Department of Physiology, Cardiovascular Research Institute, University of California, San Francisco, San Francisco, CA
[2]Department of Diabetes Complications and Metabolism, Beckman Research Institute of City of Hope, Duarte, CA

Corresponding author: Biao Wang, biao.wang@ucsf.edu.

Received 9 March 2017 and accepted 30 August 2017.

This article contains Supplementary Data online at http://diabetes.diabetesjournals.org/lookup/suppl/doi:10.2337/db17-0296/-/DC1.

Y.Wa. and E.P. contributed equally to this work.

D.W. is currently affiliated with the Institute of Molecular Medicine, Peking-Tsinghua Center for Life Sciences, Peking University, Beijing, China.

catecholamine secretion by adrenal chromaffin cells in patients with pheochromocytoma also causes extensive beige adipocyte formation (18). Additionally, increasing βAR signaling by overexpressing Adrb1 could promote beige adipocyte formation (19). Human UCP1$^+$ adipocytes are found in individuals exposed to cold environment, but their appearances are negatively correlated with aging and obesity; this feature resembles the plasticity of beige adipocytes in mice (20–24). Therefore, increasing beige adipocyte abundance has been considered as an attractive approach to promote metabolic health.

Besides the beige adipocyte population observed in adult mice, substantial amounts of beige adipocytes are present in 3-week-old pups during postnatal development (22). However, the relationship between beige adipocytes formed postnatally and upon cold stimulation in adult stage is not determined. We have found that the beige adipocytes formed postnatally gradually lost their beiging properties in adulthood, and cold stimulation can induce restoration of their beiging properties, a process we termed beige adipocyte renaissance. Liver kinase b1 (Lkb1) and salt-inducible kinases (SIKs) suppressed βAR-induced histone deacetylase 4 (Hdac4) signaling in hepatocytes (25,26) and fat body in *Drosophila* (26,27), although their roles in beige adipocyte homeostasis are unknown. In this study, we showed that, specifically, deletion of Lkb1 in adipocytes, not in brown and beige adipocytes themselves, led to a sustained beige adipocyte population regardless of βAR stimulation. Furthermore, loss of adipocyte Hdac4 in adipocyte Lkb1 knockout (Lkb1^{AKO}) mice reversed the persistent beige adipocyte expansion phenotype. Lkb1^{AKO} mice were protected against high-fat diet (HFD)–induced obesity and insulin resistance. However, these metabolic benefits were not because of expanded beige adipocytes or Ucp1-dependent thermogenesis. Our results reveal that white adipocytes play an important role in beige adipocyte maintenance, and further studies are warranted to investigate whether targeting beige adipocyte renaissance could improve metabolic homeostasis.

RESEARCH DESIGN AND METHODS

Mice

All animal experiments were approved by the University of California, San Francisco Institutional Animal Care and Use Committee in adherence to National Institutes of Health guidelines and policies. Adiponectin-Cre (JAX#010803), Rosa-iDTR (JAX#007900), and Lkb1$^{f/f}$ (JAX#014143) were obtained from The Jackson Laboratory. Hdac4$^{f/f}$ and Ucp1-Cre (JAX#024670) mice were provided by Drs. Eric Olson and Evan Rosen. Mice were in the C57Bl/6J background, and both sexes were analyzed in this study. Additional mice were described in the experimental procedures section of the Supplementary Data.

Beige Adipocyte Ablation

Three-week-old male or female mice were administrated with a single diphtheria toxin (DT) injection intraperitoneally at the dose of 10–25 ng/mouse (Biological Laboratories Inc.).

Accession Numbers

The accession number for RNA-sequencing (RNA-seq) data reported in the article is Gene Expression Omnibus GSE85335.

RESULTS

Beige Adipocytes Formed Postnatally Perdure but Lose Beiging Characteristics in Adulthood

In iWAT, *Ucp1* expression was absent in the early postnatal period (<2 weeks of age). However, it reached a peak in 3-week-old pups and gradually reduced to baseline in 8-week-old adult mice. Cold stimulation could restore *Ucp1* expression (Fig. 1*A*) (22,28). Immunoblots confirmed the gradual decline of Ucp1 protein levels from 3 to 8 weeks of age and the reappearance after 7-day cold stimulation in 8-week-old mice (Fig. 1*B*). *Ucp1* expression correlated with beige adipocyte abundance; hematoxylin and eosin (H&E) staining and Ucp1 immunostaining confirmed that ~30% of cells were the multilocular beige adipocytes in 3-week-old pups and cold-treated adult mice (Fig. 1*C* and Supplementary Fig. 1*A* and *B*), consistent with a previous report (24). These beige adipocytes formed during postnatal development were referred as postnatal beige adipocytes. To trace the fate of postnatal beige adipocytes in iWAT, we performed Ucp1 immunofluorescence staining on Ucp1-Cre; Rosa-mT/mG mice, in which past and current Ucp1$^+$ adipocytes were permanently labeled with membrane-targeted green fluorescent protein. At 1 week of age, Ucp1-Cre was not expressed in iWAT, indicated by the absence of GFP$^+$ or Ucp1$^+$ cells (Fig. 1*D*). In contrast, all brown adipocytes in iBAT were GFP$^+$ (meaning Ucp1$^+$), whereas white adipocytes in epididymal WAT (eWAT) were GFP$^-$ (meaning Ucp1$^-$) (Supplementary Fig. 1*C* and *D*). At 3 weeks of age, ~30% of cells in iWAT were GFP$^+$;Ucp1$^+$ with multilocular morphology (Fig. 1*E* and *G*). Although these GFP$^+$ cells were still present in adults (at 8 weeks of age), they were no longer Ucp1$^+$ anymore (Fig. 1*F* and *G*), suggesting that the postnatal beige adipocytes in iWAT lost their beiging characteristics in the adult stage. Although ambient temperature and nutrient status from birth to weaning can temporally affect the abundance of postnatal beige adipocytes, the responsiveness of cold-induced beige adipocyte expansion in adulthood remains intact (29,30), suggesting that the plasticity of postnatal beige adipocytes is genetically controlled.

Beige Adipocyte Renaissance: Restoring Beiging Characteristics in Postnatal Beige Adipocytes in Response to Cold

Beige adipocytes can reappear in iWAT of adult mice under βAR stimulation (16,31). For example, 8°C cold stimulation for 1 week drastically increased *Ucp1* expression and induced the formation of multilocular beige adipocytes in iWAT (Fig. 1*A* and *C*). Next, we used an Ucp1-Cre inducible DT receptor (iDTR)–mediated cell ablation system (32) (Fig. 2*A*) to determine whether postnatal beige adipocytes and cold-induced beige adipocytes were the same cell population.

In this system, current and past Ucp1$^+$ adipocytes express iDTR and can be ablated by DT injection. The *iDTR* expression correlated with *Ucp1* expression in iWAT of Ucp1-Cre; Rosa-iDTR (abbreviated as Cre$^+$) pups until 3 weeks of age (Supplementary Fig. 2*A* and *B*). However, *iDTR* retained, whereas *Ucp1* dropped to baseline in 8-week-old mice (Supplementary Fig. 2*A* and *B*), which was consistent with the observations in Ucp1-Cre;Rosa-mT/mG lineage tracing experiments (Fig. 1*D–F*). In 3-week-old Cre$^+$ pups, 3-day post-DT administration successfully ablated beige adipocytes, as *Ucp1*, *Cidea*, and *Cox8b* mRNA levels were significantly reduced in iWAT (Fig. 2*B*). Ucp1 protein levels in iWAT were also reduced after DT administration (Fig. 2*C*). Indeed, the ratios of lipid droplets to nuclei correlated with *Ucp1* mRNA levels in iWAT before or after DT administration (Fig. 2*B* and Supplementary Fig. 3*B*), confirming that multilocular Ucp1$^+$ beige adipocytes were ablated in iWAT. The thermogenic gene expression in iWAT remained low at 8 weeks of age (Fig. 2*C*), and the beige adipocytes were absent in iWAT by H&E staining and perilipin immunohistochemistry (Fig. 2*D* and Supplementary Fig. 3*A*). Moreover, increased macrophage markers *Arg1*, *Cd68*, and *Emr1* in iWAT were only evident in the 3-day post-DT group (absent in 5-week post-DT group) (Supplementary Fig. 4*A*), suggesting there was transient macrophage infiltration after DT-induced beige adipocyte ablation in iWAT.

Ucp1-Cre was also active in brown adipocytes in iBAT. Indeed, Cre$^+$ mice had increased macrophage infiltration and reduced *Ucp1* expression in iBAT 3-day post-DT administration, and their core temperature dropped 8°C during the first hour of cold exposure (Supplementary Figs. 4*B* and 5*A–C*). However, 1 week post-DT injection, *Ucp1* expression went back to normal levels in Cre$^+$ mice (Supplementary Fig. 5*C* and *D*), and they regained cold resistance (Supplementary Fig. 5*B–D*). Histology analysis also revealed a progressive regeneration of iBAT (Supplementary Fig. 5*E*). Thus, iBAT exhibited rapid regeneration upon ablation. The differential responses of brown and beige adipocytes after ablation may be because of the fact that iBAT is the first defense mechanism for hypothermia. Once a functional iBAT has been regenerated, there is no need to regenerate beige adipocyte for the thermogenic purpose. Therefore, the Ucp1-Cre;Rosa-iDTR ablation model offers us an opportunity to specifically manipulate postnatal beige adipocytes in vivo.

We then used this ablation model to address the contribution of postnatal beige adipocytes to cold-induced beige adipocyte expansion in adult mice. We administered

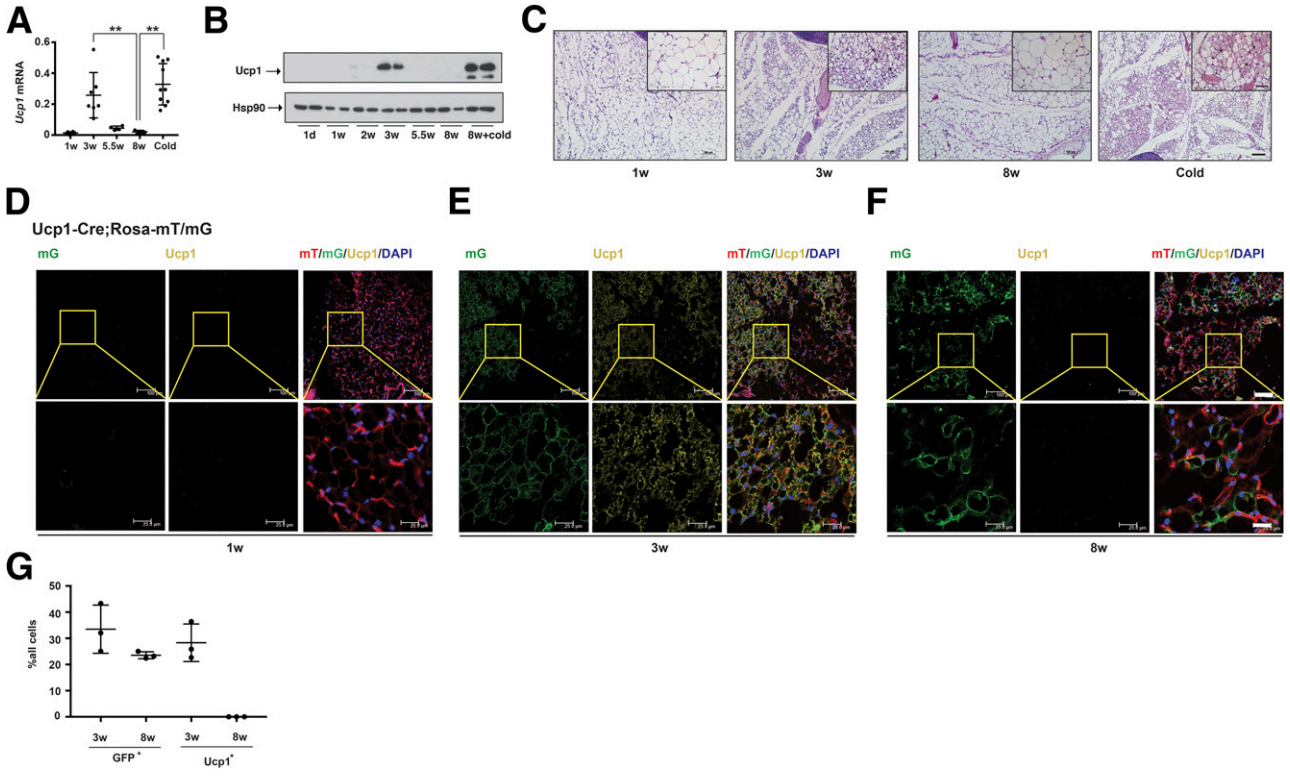

Figure 1—Beige adipocyte dynamics in iWAT. *A*: Quantitative PCR analysis of *Ucp1* mRNA levels in iWAT from wild-type B6 male and female mice at different ages and under 8°C cold treatment. n = 3–10. *B*: Immunoblots showing protein amounts of Ucp1 and Hsp90 in iWAT from B6 male and female mice at different ages. *C*: Representative H&E staining of iWAT from 1-, 3-, and 8-week-old mice and after 7-day 8°C cold treatment. Insets: arrows showing multilocular beige adipocytes. Scale bar: 50 μm. Confocal images of membrane GFP (mG), membrane Tomato (mT), and Ucp1 (by immunostaining) in iWAT from 1- (*D*), 3- (*E*), and 8- (*F*) week-old Ucp1-Cre;Rosa-mT/mG mice. Yellow boxed inserts are shown at higher magnification below each image. Scale bars: 100 μm (20 μm for inserts). *G*: Statistics of GFP$^+$ and Ucp1$^+$ adipocytes at 3 and 8 weeks of age. Student t test: $^{**}P < 0.01$.

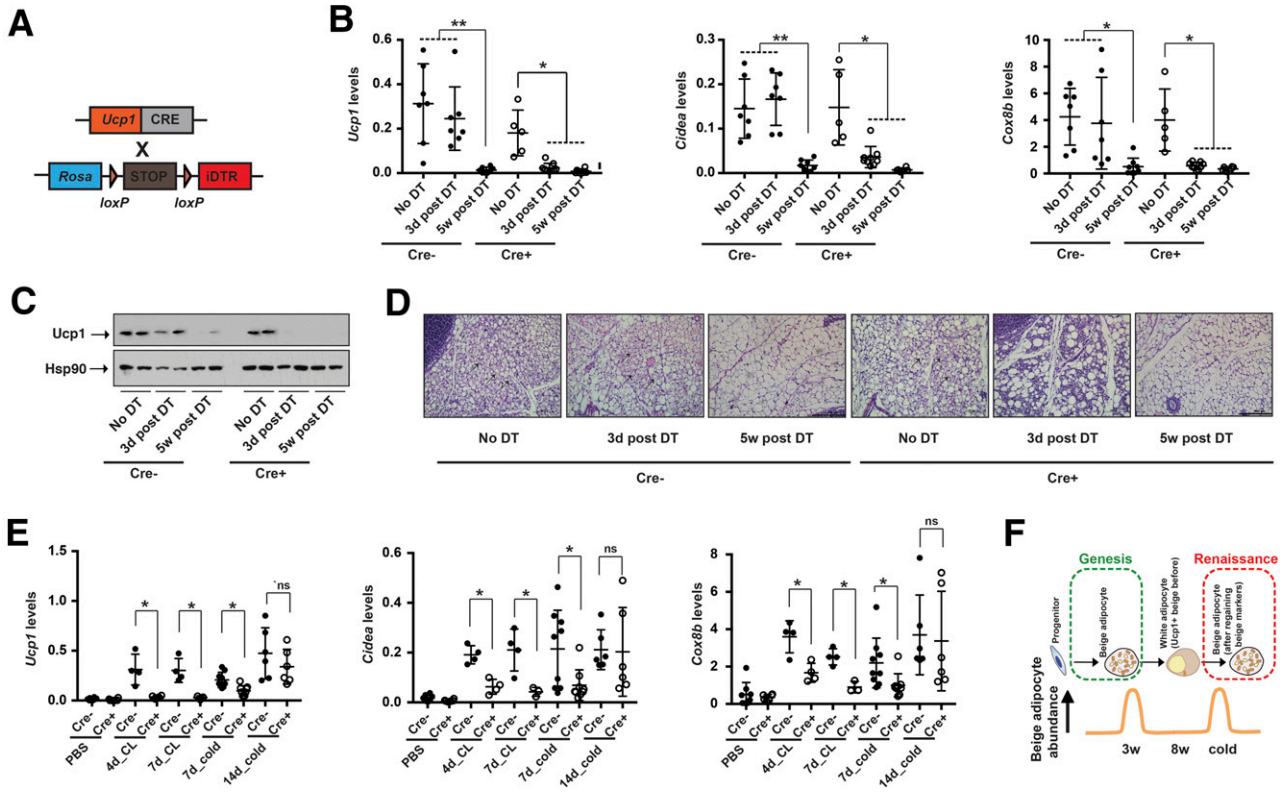

Figure 2—Beige adipocyte renaissance in response to cold in adult mice. *A*: Schematic of the beige adipocyte ablation mouse model. Ucp1-Cre mice were crossed with Rosa-iDTR mice to generate Ucp1-Cre;Rosa-iDTR mice. *B*: Quantitative PCR analysis of mRNA levels of thermogenic genes *Ucp1*, *Cidea*, and *Cox8b* in iWAT from Rosa-iDTR (Cre^-) and Ucp1-Cre;Rosa-iDTR (Cre^+) mice before and post-DT administration. DT was injected at 3 weeks of age. Sample sizes: No DT Cre^- ($n = 5$), No DT Cre^+ ($n = 4$), 3 days (3d) post-DT Cre^- ($n = 13$), 3d post-DT Cre^+ ($n = 8$), 5 weeks (5w) post-DT Cre^- ($n = 6$), and 5w post-DT Cre^+ ($n = 6$). Both male and female mice were used. *C*: Immunoblots of Ucp1 and Hsp90 in iWAT from Cre^- and Cre^+ mice at indicated time points. *D*: Representative H&E staining of iWAT from Cre^- and Cre^+ mice at indicated time points. Scale bar: 200 μm. Arrows: multilocular beige adipocytes. *E*: Quantitative PCR analysis of *Ucp1*, *Cidea*, and *Cox8b* mRNA levels in iWAT from ∼8-week-old male and female Cre^- and Cre^+ mice treated with PBS or CL (0.2 mg/kg for 4 consecutive days or 1 mg/kg for 7 consecutive days) for 7 or 14 days at 8°C. DT was injected at 3 weeks of age. Sample sizes: PBS Cre^- ($n = 6$), PBS Cre^+ ($n = 4$), 4 days (4d)_CL Cre^- ($n = 5$), 4d_CL Cre^+ ($n = 5$), 7 days (7d)_CL Cre^- ($n = 6$), 7d_CL Cre^+ ($n = 4$), 7d_Cold Cre^- ($n = 9$), 7d_Cold Cre^+ ($n = 9$), 14 days (14d)_Cold Cre^- ($n = 6$), and 14d_Cold Cre^+ ($n = 6$). *F*: Diagram showing the life of beige adipocyte. Genesis refers to de novo beige adipocyte formation from progenitors during postnatal phase, whereas renaissance refers to the process of once $Ucp1^+$ white adipocytes regaining beiging properties (Ucp1 and other thermogenic gene expression and multilocular morphology) upon cold in adult mice. Student *t* test: ns, not significant; $^*P < 0.05$; $^{**}P < 0.01$.

DT in Cre^- and Cre^+ mice at 3 weeks of age to ablate postnatal beige adipocytes, followed by injection of CL316243 (a β3-specific agonist [CL]) for 4 or 7 consecutive days at 8 weeks of age. Although CL strongly induced *Ucp1*, *Cidea*, and *Cox8b* mRNA levels in iWAT from Cre^- mice, its effect in beige-ablated Cre^+ mice was attenuated (Fig. 2*E*). This observation indicated that CL restored *Ucp1* and expression of other thermogenic genes in postnatal beige adipocytes. A similar result was obtained in 7-day 8°C cold stimulation (Fig. 2*E*). However, longer cold stimulation (14 days at 8°C) did induce *Ucp1* expression in beige-ablated Cre^+ mice (Fig. 2*E*). This could be because of induction of beige adipocyte adipogenesis from progenitors in adult mice (33–35), which might occur independently of beige adipocyte renaissance. The $Pdgfr\alpha^+Sca1^+$ progenitors were responsible for cold-induced beige adipocyte adipogenesis (31,36). These progenitors were present in iWAT and iBAT before and after beige adipocyte ablation (Supplementary Fig. 6*A* and *B*), suggesting that they may contribute to the cold-induced beige adipocyte adipogenesis in iWAT and BAT regeneration after DT-mediated ablation. In contrast, both CL and cold induced eWAT *Ucp1* expression similarly in postnatal beige adipocyte ablated and nonablated mice (Supplementary Fig. 7), suggesting the involvement of de novo adipogenesis in cold-induced beige adipocyte formation in epididymal fat depot.

Collectively, there are two consecutive waves of beige adipocyte formation in iWAT; the first one is because of de novo adipogenesis (genesis) during postnatal development and peaks at 3 weeks of age, and the other one is through restoring the beige characteristics in the postnatal beige adipocytes by βAR stimulation at adult stage (renaissance) (Fig. 2*F*). Notably, beige adipocyte renaissance and de novo beige adipogenesis are not mutually exclusive; thus, new beige adipocytes did form in response to cold in beige-ablated mice, but to a lower degree.

SIKs and Lkb1 Suppress Beige Adipocyte Renaissance

βAR stimulation elevates secondary messenger cyclic adenosine monophosphate/cAMP levels and induces transcriptional program in target cells. Previously, we have shown that SIKs, a family of AMPK-related kinases, suppress cAMP-induced transcriptional program by phosphorylation and inhibition of two distinct classes of transcription cofactors: CREB-regulated transcription coactivators and class IIa HDACs (26,37,38). This SIK-dependent regulation of cAMP transcriptional response is conserved in *Caenorhabditis elegans*, *Drosophila*, and mammals, and all SIK members contain a conserved cAMP-dependent protein kinase (PKA) phosphorylation site at their COOH-terminal (25,39) (Supplementary Fig. 8*A* and *B*). Mammalian SIK family contains three members: Sik1, -2, and -3. Sik2 was highly expressed in mature adipocytes compared with stromal vascular fraction cells from various depots, whereas Sik1 and Sik3 were expressed at lower levels in mature adipocytes (Supplementary Fig. 8*C*). Although roles of SIKs in adipose have been explored (40,41), whether SIKs regulate beige adipocyte formation remains unknown. We investigated thermogenic gene expression in iWAT from SIK-deficient animals. Neither Sik1 nor Sik2 global KO mice exhibited obvious changes in *Ucp1* expression in iWAT (data not shown), reflecting functional compensation between SIK members. However, we did observe elevated *Ucp1* expression in iWAT of 8-week-old Sik1;Sik2 KO mice without affecting PKA signaling (Supplementary Fig. 8*D* and *E*), suggesting that SIKs were downstream components of βAR signaling, and they suppressed *Ucp1* expression in iWAT. In contrast, adipocyte AMPK-deficient mice exhibited attenuated browning potential in response to CL stimulation in iWAT (42), suggesting that AMPK and SIKs differentially regulated beige adipocyte expansion in iWAT.

Because the Sik1;Sik2 KO mice used in this study were global KO models, we could not rule out the possibility that SIK deficiency in other tissues contributed to beige adipocyte renaissance in iWAT. We and others (26,27) have shown that liver kinase b1/Lkb1-mediated phosphorylation of a conserved Thr residue in the activating loop of SIK kinase domain was required for SIK activation. We used Adiponectin-Cre to generate Adiponectin-Cre;Lkb1$^{f/f}$ (Lkb1^{AKO} mice), in which Lkb1 was specifically deleted in adipose tissues, such as iBAT, iWAT, and eWAT (Supplementary Fig. 9*A*). Lkb1 expression in other tissues (liver, spleen, kidney, lung, brain, gut, and heart) was not affected (Supplementary Fig. 9*B*). AMPK is another known Lkb1 substrate, and AMPK and its substrate ACC were hypophosphorylated in iWAT of Lkb1^{AKO} mice (Supplementary Fig. 9*B*), confirming the absence of Lkb1 signaling in iWAT of Lkb1^{AKO} mice. We also use Ucp1-Cre to generate Ucp1-Cre; Lkb1$^{f/f}$ (Lkb1^{BKO} mice) to delete Lkb1 in brown and beige adipocytes only. We did not observe a difference in Ucp1 expression or beige adipocyte abundance in 3-week-old Lkb1^{AKO} and Lkb1^{BKO} pups (Fig. 3*A*–*C* and Supplementary Fig. 10*B*). We further investigated whether Lkb1 deletion in adipocytes affects beige adipocyte homeostasis in adult mice. At ~8 weeks of age, Lkb1^{AKO} mice exhibited an increase of Ucp1 mRNA and protein levels and a substantial population of beige adipocytes in iWAT compared with control mice (Fig. 3*A*–*C*). Other thermogenic genes (*Cox8b*, *Cidea*, and *Dio2*) were also elevated in iWAT (Supplementary Fig. 10*A*). In contrast, increased Ucp1 expression and expanded beige population in iWAT were not observed in adult Lkb1^{BKO} mice (Fig. 3*A* and Supplementary Fig. 10*B*).

Constant βAR stimulation is necessary to induce and sustain beige adipocyte population in rodents and humans. As shown in Fig. 3*D*, 4-day consecutively intraperitoneal injection of CL induced *Ucp1* expression and beige adipocyte formation, and this effect was lost after 4-day recovery period (without CL). Surprisingly, the CL administration did not further increase iWAT *Ucp1* expression in Lkb1^{AKO} mice, and *Ucp1* expression was not diminished during the recovery phase (Fig. 3*D*). Similarly, iWAT *Ucp1* expression in Lkb1^{AKO} mice was largely unchanged upon either cold stimulation (8°C for 7 days) or withdrawn from the cold environment (7 and 14 days at room temperature after 8°C cold stimulation) (Fig. 3*D* and *F*). Hence, beiging characteristics of beige adipocytes, transient in nature, were persistently present in Lkb1^{AKO} mice regardless of cold stimulation. Furthermore, this persistent beige adipocyte expansion did not require Lkb1 signaling in beige adipocytes themselves, as Lkb1^{BKO} mice showed dynamic beige adipocyte profile similar to control mice (Fig. 3*E*). Therefore, Lkb1 deficiency in white adipocytes led to persistent beige adipocyte renaissance in adult mice noncell autonomously. In the same setting, *Ucp1* expression in eWAT was upregulated by CL and dropped to baseline after recovery in both Lkb1^{AKO} and control mice, suggesting there are two different mechanisms for cold-induced beige adipocyte formation in iWAT and eWAT (Supplementary Fig. 10*C*).

Notably, iWAT *Ucp1* expression declined in Lkb1^{AKO} mice after 2 weeks on thermoneutrality (Fig. 4*A*), suggesting that the absence of cold-induced sympathetic nervous system (SNS) activity totally blocked beige adipocyte formation in Lkb1^{AKO} mice. However, there was no change of PKA activity in iWAT from Lkb1^{AKO} mice (also in Lkb1^{BKO} mice) at 8 weeks of age at room temperature (Fig. 4*B*), suggesting that the appearance of beige adipocytes in Lkb1^{AKO} mice was not because of an increase of SNS activity in iWAT. This observation was also further confirmed by no changes in tissue catecholamine levels (Fig. 4*C*) or sympathetic nerve density (by tyrosine hydroxylase immunostaining) in iWAT of Lkb1^{AKO} mice (Fig. 4*D* and *E*). Collectively, at thermoneutrality (with no thermal stress), there is no beige adipocyte in both control and Lkb1^{AKO} mice, because of lack of SNS activity and catecholamines, whereas at room temperature (with mild thermal stress for mice), Lkb1 deficiency in white adipocytes augments intracellular PKA-dependent transcriptional response and triggers beige adipocyte expansion in iWAT without increasing upstream PKA activity. Therefore, Lkb1 is functioning as a brake to suppress βAR–PKA signaling in white adipocyte during beige adipocyte renaissance.

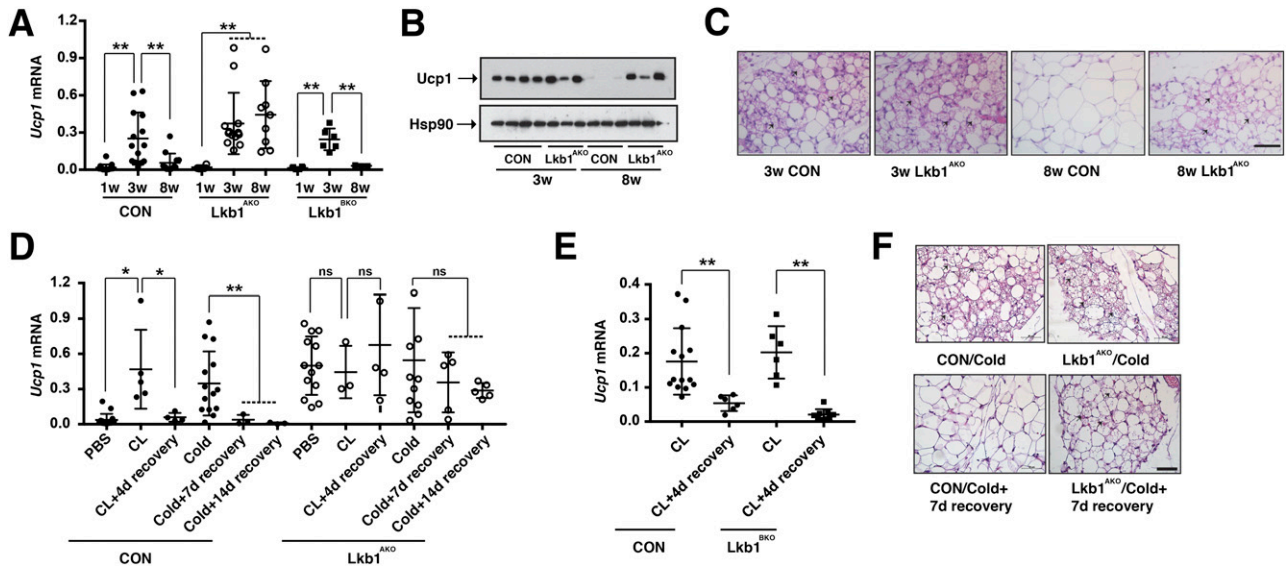

Figure 3—Lkb1 in white adipocyte suppresses beige adipocyte renaissance. *A*: Quantitative PCR (q-PCR) analysis of *Ucp1* mRNA levels in iWAT from male Lkb1$^{f/f}$ (CON), Lkb1^{AKO}, and Lkb1^{BKO} mice at 1, 3, and 8 weeks of age. Sample sizes: 1w) CON (n = 17), 1w Lkb1^{AKO} (n = 4), 1w Lkb1^{BKO} (n = 6), 3w CON (n = 14), 3w Lkb1^{AKO} (n = 13), 3w Lkb1^{BKO} (n = 2), 8w CON (n = 12), 8w Lkb1^{AKO} (n = 9), and 8w Lkb1^{BKO} (n = 3). *B*: Immunoblots showing protein amounts of Ucp1 and Hsp90 in iWAT from 3- and 8-week-old male CON and Lkb1^{AKO} mice. *C*: Representative H&E staining of iWAT from 3- and 8-week-old CON and Lkb1^{AKO} male mice. Scale bar: 50 μm. *D*: q-PCR analysis of *Ucp1* mRNA levels in iWAT from 8-week-old male and female CON and Lkb1^{AKO} mice at different conditions. CL: 0.2 mg/kg for 4 days; CL+4d recovery: CL injections followed by 4 days without CL; Cold: 8°C for 7 days; Cold+7d (or 14d) recovery: 8°C cold followed by 7 (or 14) days at room temperature. Sample sizes: PBS CON (n = 16), PBS Lkb1^{AKO} (n = 13), CL CON (n = 5), CL Lkb1^{AKO} (n = 3), CL+4d recovery CON (n = 4), CL+4d recovery Lkb1^{AKO} (n = 5), Cold CON (n = 14), Cold Lkb1^{AKO} (n = 10), Cold+7d recovery CON (n = 3), Cold+7d recovery Lkb1^{AKO} (n = 5), Cold+14d recovery CON (n = 3), and Cold+14d recovery Lkb1^{AKO} (n = 5). *E*: q-PCR analysis of *Ucp1* mRNA levels in iWAT from 8-week-old male and female CON and Lkb1^{BKO} mice after CL and CL plus 4-day recovery conditions. Sample sizes: CL CON (n = 14), CL Lkb1^{BKO} (n = 6), CL+4d recovery CON (n = 6), and CL+4d recovery Lkb1^{BKO} (n = 9). *F*: Representative H&E staining of iWAT from 8-week-old male CON and Lkb1^{AKO} mice at cold and cold plus 7-day recovery conditions. Scale bar: 50 μm. Arrows indicate multilocular beige adipocytes. Student t test: ns, not significant; $^*P < 0.05$; $^{**}P < 0.01$.

Lkb1 Suppresses Beige Adipocyte Renaissance Through Hdac4 Inhibition

We and others (26) have shown that deletion of class IIa HDAC4 fully rescued phenotypes of SIK3 and Lkb1 mutants in *Drosophila*. Indeed, we observed that CL stimulation induced Sik2 phosphorylation at Ser^{587} and Hdac4 dephosphorylation at Ser^{245} in iWAT (Fig. 5*A*). Hdac4 was also hypophosphorylated in adipocytes from iWAT of Lkb1^{AKO} mice (Fig. 5*B*). We then examined whether adipocyte class IIa Hdac4 activation was required for beige adipocyte expansion in Lkb1^{AKO} mice. The adipocyte Lkb1;Hdac4 double KO (abbreviated as Lkb1;Hdac4^{AKO}) mice had no expanded beige adipocytes in iWAT, similar to wild-type and adipocyte Hdac4 KO (Adiponectin-Cre;Hdac4$^{f/f}$, abbreviated as Hdac4^{AKO}) mice (Fig. 5*C*). In addition, Lkb1;Hdac4^{AKO} mice regained responsiveness to cold and cold plus recovery regarding *Ucp1* expression, similar to wild-type and Hdac4^{AKO} mice (Fig. 5*D*). Furthermore, RNA-seq analysis revealed that 436 genes were upregulated in iWAT of 8-week-old Lkb1^{AKO} mice at normal chow (NC), and ~40% of these genes were regulated in an Hdac4-dependent fashion (Fig. 5*E* and *F* and Supplementary Table 2). The top five gene ontology categories of Hdac4-dependent transcripts that were upregulated in Lkb1^{AKO} mice included mitochondrial metabolic and muscle development processes (Fig. 5*G*). We further confirmed that adipocyte Hdac4 deficiency rescued or partially rescued elevated expression levels of some thermogenic signature genes (including *Ucp1*, *Dio2*, and *Cidea*) and metabolic genes (including *Cox7a1*, *Acaa2*, *Gyk*, *Ldhd*, and *Scl27a1*) in Lkb1^{AKO} mice (Fig. 5*H*). All data in this study suggest that Hdac4 is indeed a key downstream component of Lkb1 signaling in adipocytes regulating beige adipocyte renaissance in iWAT.

Lkb1^{AKO} Mice Exhibit Improved Metabolic Performance Under HFD Regardless of Beige Adipocyte Expansion and Ucp1-Mediated Thermogenesis

We next investigated whether deletion of Lkb1 in adipocytes affected metabolic performance. We did not observe noticeable metabolic changes in Lkb1^{AKO} mice under NC condition. Compared with controls, Lkb1^{AKO} mice had identical growth rates until ~6 months of age, similar fasting glucose, and insulin sensitivity (Supplementary Fig. 11*A*–*C*). In vitro lipolysis rate and CL-induced free fatty acid release in vivo were not affected in Lkb1^{AKO} mice (Supplementary Fig. 11*D* and *E*), which was consistent with previous observation that PKA activity was not altered in Lkb1^{AKO} mice (Fig. 4*B*). Comprehensive Lab Animal Monitoring System (CLAMS) studies indicated that Lkb1^{AKO} mice had similar energy expenditure, respiratory exchange ratio, food intake,

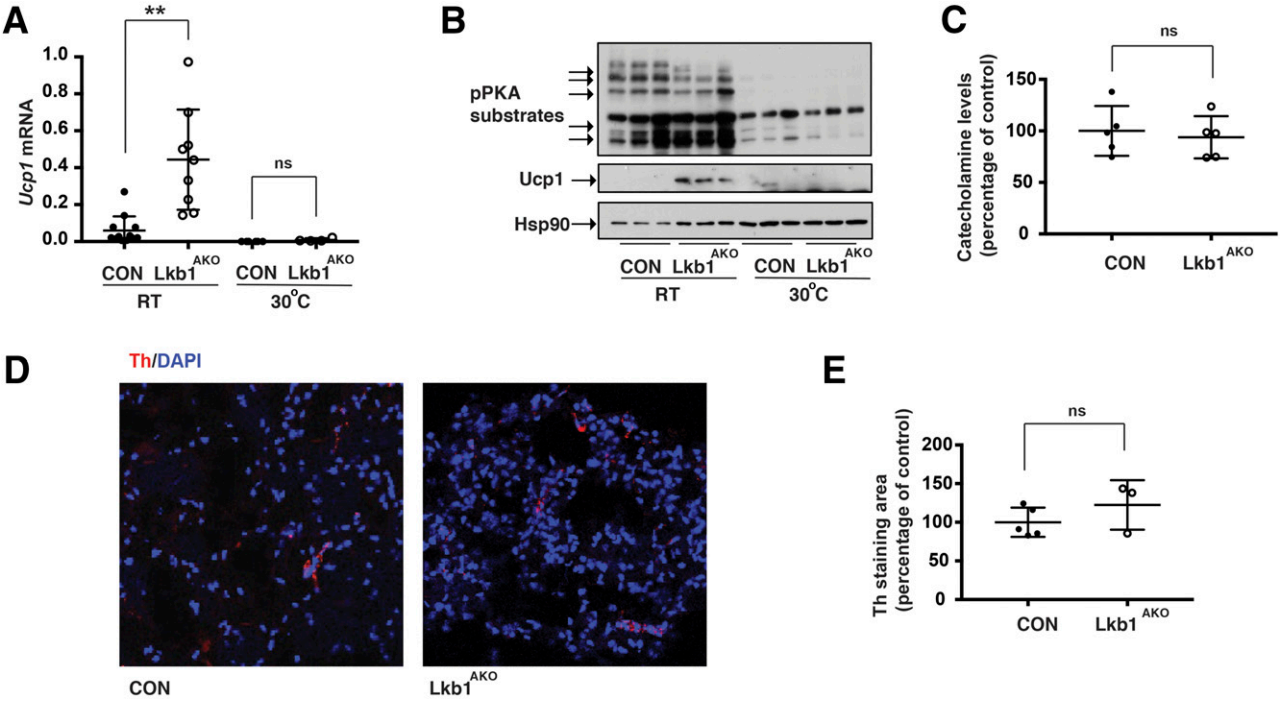

Figure 4—Sympathetic activities in iWAT of Lkb1^{AKO} mice. *A*: Quantitative PCR analysis of *Ucp1* mRNA levels in iWAT from 8-week-old male Lkb1$^{f/f}$ (CON) and Lkb1^{AKO} mice housed at room temperature (RT) and thermoneutral conditions. Sample sizes: CON/RT (n = 12), Lkb1^{AKO}/RT (n = 9), CON/30°C (n = 6), and Lkb1^{AKO}/30°C (n = 4). *B*: Immunoblots of phosphorylated (p-)PKA substrates, Ucp1, and Hsp90 in iWAT from ~8-week-old male CON and Lkb1^{AKO} mice housed at RT or 30°C. *C*: Relative iWAT tissue catecholamine levels in ~8-week-old male CON and Lkb1^{AKO} mice. Sample sizes: CON (n = 5) and Lkb1^{AKO} (n = 5). Representative tyrosine hydroxylase (Th) immunostaining (*D*) and counts of Th^{+} fibers (*E*) in iWAT from ~8-week-old male CON and Lkb1^{AKO} mice. Student t test: ns, not significant; $^{**}P < 0.01$.

physical activity, and other parameters compared with their control littermates (Supplementary Fig. 12*A–L*).

HFD feeding can whiten the beige adipocyte. Interestingly, the beige adipocyte population in Lkb1^{AKO} mice even persisted after 4 to 5 weeks of HFD feeding (Fig. 6*A* and *B*). In fact, enhanced expression of thermogenic genes *Ucp1*, *Dio2*, and *Pgc1α* in both NC and HFD conditions was also observed through screening of the expression levels of ~200 key genes involved in adipogenesis and lipid metabolism pathways (Supplementary Fig. 13*A*). Furthermore, the thermogenic gene signature identified by RNA-seq from Lkb1^{AKO} mice at NC was also present after HFD (Supplementary Fig. 13*B*). Because substantial beige adipocyte population was absent in Lkb1^{BKO} mice (Fig. 6*A* and *B*), we then compared metabolic performance of Lkb1^{AKO} and Lkb1^{BKO} mice under short-term HFD. Surprisingly, both Lkb1^{AKO} and Lkb1^{BKO} mice showed reduced weight gain under HFD and similar insulin resistance (Fig. 6*C–E*). CLAMS studies of Lkb1^{AKO} mice after HFD showed no differences in organismal oxygen consumption (when normalized per lean body weight or per animal), respiratory exchange ratio, and food intake (Supplementary Fig. 14*A–C*), although there was a slight increase of physical activities (Supplementary Fig. 14*D–F*). There were no differences in fasting glucose, serum insulin, and free fatty acid levels in Lkb1^{AKO} mice under short-term HFD (Supplementary Fig. 15*A–C*).

We have shown previously that Hdac4 was required for beige adipocyte expansion in Lkb1^{AKO} mice. Lkb1;Hdac4^{AKO} mice did not have expanded beige adipocytes (Fig. 5*C* and *D*); however, they still showed reduced adiposity and improved insulin sensitivity (Fig. 6*F–H*). No differences were observed in Hdac4^{AKO} mice compared with control mice. Therefore, beige adipocytes do not contribute to metabolic benefits in Lkb1^{AKO} mice.

To further determine whether Ucp1-mediated adaptive thermogenesis was required for adiposity phenotype of Lkb1^{AKO} mice under HFD, we then generated Lkb1^{AKO} mice in Ucp1 KO background (Lkb1^{AKO};Ucp1 KO mice). Lkb1^{AKO};Ucp1 KO mice still maintained multilocular beige adipocytes in iWAT under HFD, consistent with elevated thermogenic gene expression (*Dio2*, *Cox8b*, *Cidea*, and *Pgc1a*) (Fig. 7*A* and *B*). They also showed reduced adiposity under HFD (Fig. 7*C* and *D*). Therefore, we conclude that Ucp1-dependent thermogenesis do not contribute to leanness in Lkb1^{AKO} mice under HFD. Taken together, comparison of the metabolic performance of Lkb1^{AKO} mice (with beige expansion) with Lkb1^{BKO} (without beige expansion), Lkb1;Hdac4^{AKO} (without beige expansion), and Lkb1^{AKO};Ucp1 KO mice (without Ucp1-mediated adaptive thermogenesis) further suggests that neither beige adipocytes nor Ucp1-dependent adaptive thermogenesis contributes to metabolic benefits in Lkb1^{AKO} mice.

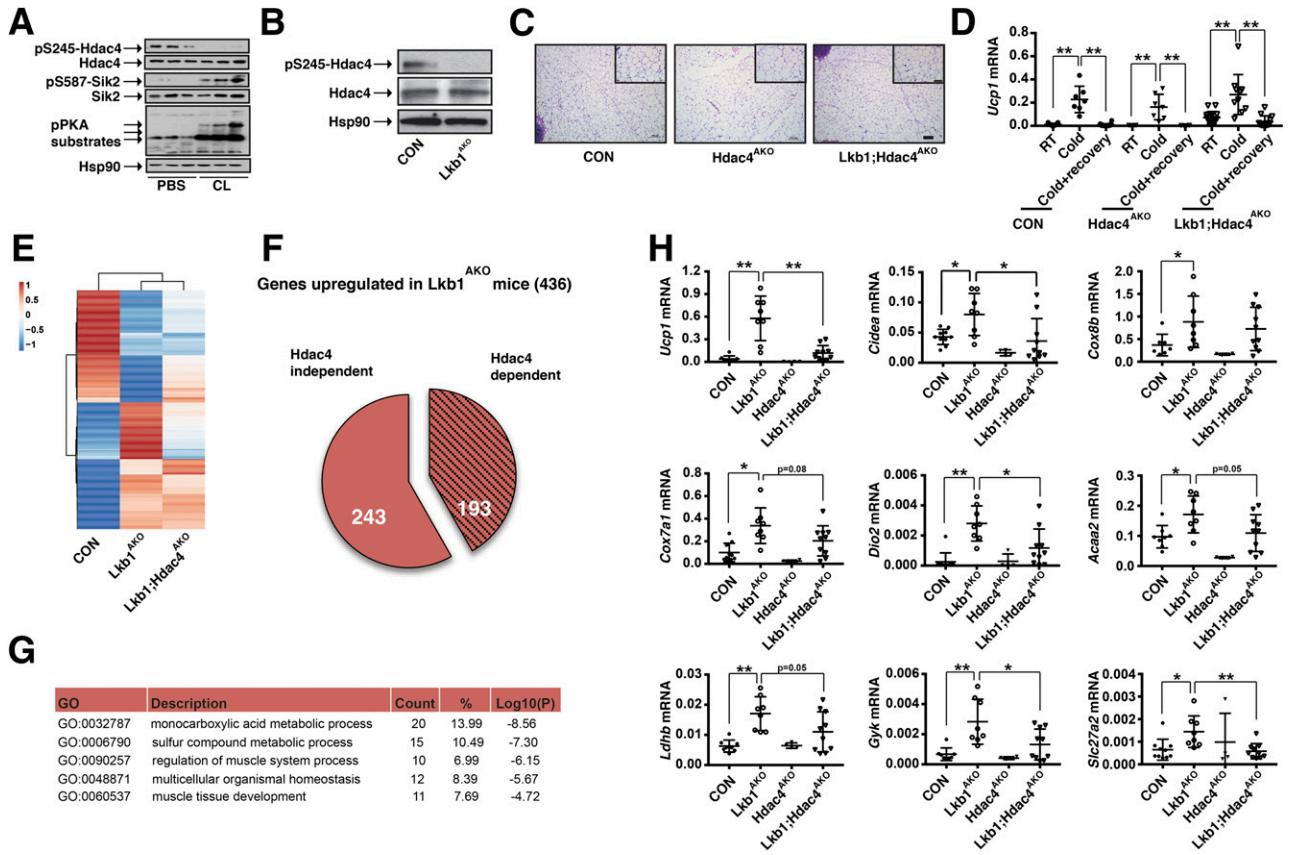

GO	Description	Count	%	Log10(P)
GO:0032787	monocarboxylic acid metabolic process	20	13.99	-8.56
GO:0006790	sulfur compound metabolic process	15	10.49	-7.30
GO:0090257	regulation of muscle system process	10	6.99	-6.15
GO:0048871	multicellular organismal homeostasis	12	8.39	-5.67
GO:0060537	muscle tissue development	11	7.69	-4.72

Figure 5—Adipocyte Hdac4 activation is required for beige adipocyte renaissance. *A*: Immunoblots showing pS245 and total Hdac4, pS587 and total Sik2, phosphorylated (p-)PKA substrates, and Hsp90 in iWAT from 8-week-old male C57Bl/6J mice, before and 30 min after 1 mg kg^{-1} CL injection. *B*: Immunoblots showing pS245 and total Hdac4 and Hsp90 in isolated iWAT adipocytes from 8-week-old male $Lkb1^{f/f}$ (CON) and $Lkb1^{AKO}$ mice. *C*: Representative H&E staining of iWAT of 8-week-old male CON, $Hdac4^{AKO}$, and $Lkb1;Hdac4^{AKO}$ mice at NC. Scale bar: 100 μm; insert scale bar: 50 μm. *D*: Quantitative PCR analysis of *Ucp1* mRNA levels in iWAT from 8-week-old male and female CON and $Lkb1;Hdac4^{AKO}$ mice. Sample sizes: room temperature (RT) CON (n = 13), RT $Hdac4^{AKO}$ (n = 4), RT $Lkb1;Hdac4^{AKO}$ (n = 14), Cold CON (n = 7), Cold $Hdac4^{AKO}$ (n = 7), Cold $Lkb1;Hdac4^{AKO}$ (n = 10), Cold+recovery CON (n = 18), Cold+recovery $Hdac4^{AKO}$ (n = 6), and Cold+recovery $Lkb1;Hdac4^{AKO}$ (n = 13). *E*: Clustering analysis and heat map of differentially expressed genes (1.5-fold up or down) of iWAT from 8-week-old male CON, $Lkb1^{AKO}$, and $Lkb1;Hdac4^{AKO}$ mice at NC housed at RT. *F*: Pie chart analysis of Hdac4 dependency of upregulated genes. *G*: List of gene ontology (GO) number, description, count, percentage, and Log10(p) value of the top five processes enriched in Hdac4-dependent genes that were upregulated in $Lkb1^{AKO}$ mice. *H*: Quantitative PCR analysis of a panel of beige adipocyte selected genes in iWAT from 8-week-old male and female CON, $Lkb1^{AKO}$, $Lkb1;Hdac4^{AKO}$, and $Hdac4^{AKO}$ mice. Sample sizes: CON (n = 10), $Lkb1^{AKO}$ (n = 8), $Hdac4^{AKO}$ (n = 4), and $Lkb1;Hdac4^{AKO}$ (n = 10). Student t test: $^*P < 0.05$; $^{**}P < 0.01$.

Lkb1 Regulates Thermogenic Capacity in iBAT Independently of Hdac4

Because $Lkb1^{BKO}$, $Lkb1^{AKO}$, and $Lkb1;Hdac4^{AKO}$ mice had Lkb1 deficiency in classic brown adipocytes, we also investigated whether adaptive thermogenesis was affected in these three mouse models. Their brown adipocyte morphology in iBAT was not significantly altered, although *Ucp1* expression in iBAT exhibited a trend of upregulation in $Lkb1^{AKO}$ and $Lkb1^{BKO}$ mice compared with controls (Supplementary Fig. 16*A* and *B*). However, $Lkb1^{AKO}$ mice were cold sensitive; they failed to maintain their core temperature in a 4°C cold tolerance test, although they could maintain their core temperature when we group-housed mice during 4°C cold challenge (Supplementary Fig. 16*C*). Hdac4 was also hypophosphorylated in iBAT of $Lkb1^{AKO}$ mice (Supplementary Fig. 16*D*). However, Hdac4 activation in BAT of $Lkb1^{AKO}$ mice did not affect Ucp1 expression (Supplementary Fig. 16*E*). The thermogenic defects in $Lkb1^{AKO}$ mice were Hdac4 independent; $Lkb1;Hdac4^{AKO}$ mice remained cold-sensitive as $Lkb1^{AKO}$ mice (Supplementary Fig. 16*F*).

Recently, Shan et al. (43) showed that $Lkb1^{AKO}$ mice exhibited enhanced adaptive thermogenesis and improved metabolic performance under HFD. The discrepancy of the role of Lkb1's deficiency on adaptive thermogenesis could originate from the use of different methodologies. For example, we used single-housed animals for cold-tolerance assay, because group-housed $Lkb1^{AKO}$ mice remained cold resistant as littermate controls (Supplementary Fig. 15*C*). Also, we normalized O_2 consumption per lean body weight or per mouse in CLAMS experiments, especially after HFD, as previously suggested in the literature (44,45). Collectively, our results suggest that Lkb1 regulates two different pathways in iWAT and iBAT; in iWAT, Lkb1 regulates beige adipocyte renaissance in an Hdac4-dependent manner

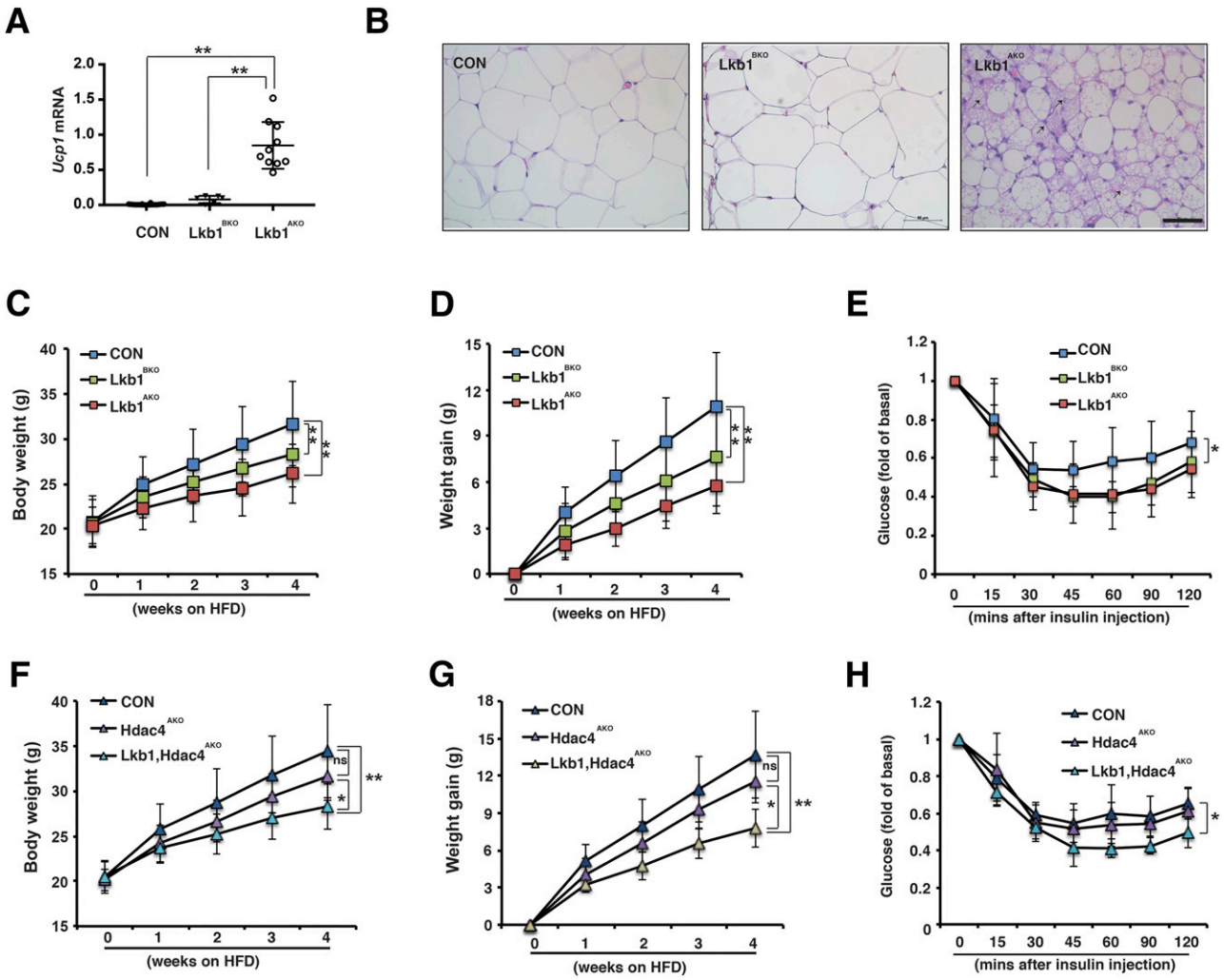

Figure 6—Adipocyte Lkb1-deficient mice exhibit improved metabolic performances under HFD independently of beige adipocyte expansion. *A*: Quantitative PCR analysis of *Ucp1* mRNA levels in iWAT from 10–12-week-old male Lkb1$^{f/f}$ (CON), Lkb1^{BKO}, and Lkb1^{AKO} mice after 4- to 5-week HFD. Sample sizes: CON (n = 18), Lkb1^{AKO} (n = 10), and Lkb1^{BKO} (n = 6). *B*: Representative H&E staining of iWAT from male CON, Lkb1^{BKO}, and Lkb1^{AKO} mice after 4- to 5-week HFD. Scale bar: 50 μm. Arrows indicate multilocular beige adipocytes. Body weight (*C*) and body weight gain (*D*) upon HFD of male CON, Lkb1^{BKO}, and Lkb1^{AKO} mice. Sample sizes: CON (n = 71), Lkb1^{BKO} (n = 30), and Lkb1^{AKO} (n = 34). *E*: Insulin tolerance tests of male CON, Lkb1^{BKO}, and Lkb1^{AKO} mice after HFD. Sample sizes: CON (n = 30), Lkb1^{AKO} (n = 28), and Lkb1^{BKO} (n = 9). Body weight (*F*) and body weight gain (*G*) upon HFD of male CON, Hdac4^{AKO}, and Lkb1;Hdac4^{AKO} mice. Sample sizes: CON (n = 13), Hdac4^{AKO} (n = 5), and Lkb1;Hdac4^{AKO} (n = 11). *H*: Insulin tolerance test of male CON and Lkb1;Hdac4^{AKO} mice after 4- to 5-week HFD. Sample sizes: CON (n = 7), Hdac4^{AKO} (n = 5), and Lkb1;Hdac4^{AKO} (n = 9). Student t test: ns: not significant; *P < 0.05; **P < 0.01.

(Fig. 8), whereas in iBAT, it controls thermogenic capacity independently of Hdac4. How Lkb1 signaling in iBAT regulates adaptive thermogenesis and energy homeostasis requires further studies.

DISCUSSION

Multiple lines of investigations have established that beige adipocytes arose from either de novo adipogenesis from progenitors or transdifferentiation from white adipocytes under various conditions (23,24,31,33,35,46). Lee et al. (24) and Contreras et al. (28) previously reported that iWAT denervation at 3 weeks of age impaired CL's ability to reinstate beige adipocyte characteristics at the adult stage. However, the underlying cellular and molecular mechanisms are not addressed. Our studies indicate that cold induces beige adipocyte renaissance in adult mice; it restores the beiging properties in the postnatal beige adipocytes, which have lost their beige properties in iWAT in adulthood. At the morphological level, our renaissance model is similar to the transdifferentiation model; both suggest a drastic white-to-beige morphology change without new adipocyte formation. However, the distinct feature of beige adipocyte renaissance is that white-like adipocyte converted to beige adipocyte by cold was once Ucp1^{+} beige adipocyte during postnatal development. Thus, not every white adipocyte in iWAT can be transdifferentiated to beige adipocyte in response to cold. Rosenwald et al. (23) had also reported that >70% of cold-induced beige adipocytes came

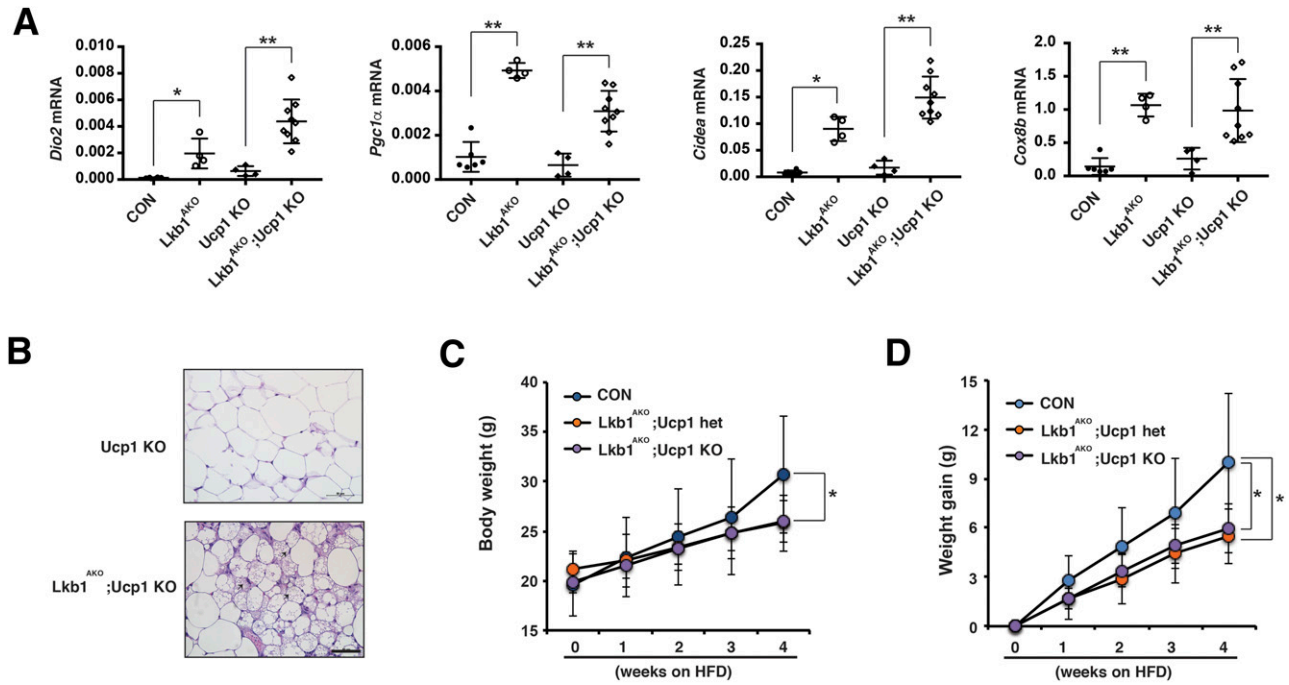

Figure 7—Ucp1-mediated adaptive thermogenesis does not contribute to metabolic benefits in Lkb1^{AKO} mice under HFD. *A*: Quantitative PCR analysis of *Dio2*, *Pgc1α*, *Cidea*, and *Cox8b* mRNA levels in iWAT from male Lkb1$^{f/f}$ (CON), Lkb1^{AKO}, Ucp1 KO, and double Lkb1^{AKO};Ucp1 KO mice after 4-week HFD. Sample sizes: CON (n = 6; genotype: Lkb1$^{f/f}$), Lkb1^{AKO} (n = 4), Ucp1 KO (n = 4; genotype: Lkb1$^{f/f}$;Ucp1 KO), and Lkb1^{AKO};Ucp1 KO (n = 9). *B*: Representative H&E staining of iWAT from male Ucp1 KO and Lkb1^{AKO};Ucp1 KO mice after 4- to 5-week HFD. Scale bar: 50 μm. Arrows indicate multilocular beige adipocytes. Body weight (*C*) and body weight gain (*D*) upon HFD of male CON, Lkb1^{AKO};Ucp1 heterozygotes (het), and Lkb1^{AKO};Ucp1 KO mice. Sample sizes: CON (n = 12, including 4 Lkb1$^{f/f}$;Ucp1 het and 8 Lkb1$^{f/f}$;Ucp1 KO), Lkb1^{AKO};Ucp1 het (n = 5), and Lkb1^{AKO};Ucp1 KO (n = 7). Student t test: $^{*}P < 0.05$; $^{**}P < 0.01$.

from white adipocytes with Ucp1-expressing memory. Based on lineage-tracing experiments using Ucp1-Cre;Rosa-mT/mG mice (Fig. 1*D*–*G*), we expected that at adult stage, ~30% of cells in iWAT were Ucp1^{+} at 3 weeks of age, and they could regain *Ucp1* expression and other beiging properties after cold stimulation. This number is in agreement with previous studies; both Lee et al. (24) and Berry et al. (35) showed 30–40% of cold-induced beige adipocytes were from preexisting white adipocytes labeled by adiponectin-Cre^{ERT2} in adult mice.

Beige adipocyte renaissance may be the default mechanism of beige adipocyte formation in iWAT, which can provide a rapid adaptive response to cold (restoring thermogenic machinery rather than generating new thermogenic adipocytes). The de novo beige adipocyte adipogenesis program can be activated under persistent cold stimulation (33) or in the absence of beige adipocyte renaissance. Interestingly, postnatal beige adipocytes may potentially stimulate recruitment of progenitors upon cold stimulation, because postnatal beige adipocyte ablation suppressed cold-induced beige adipocyte formation from progenitors (Fig. 2*F*). Notably, beige adipocyte renaissance is a depot-specific phenomenon; it does not occur in eWAT.

We further delineate an Lkb1-Hdac4–dependent mechanism in white adipocytes that governs the beige adipocyte renaissance noncell autonomously (Fig. 8). Lkb1^{AKO} mice exhibited persistent beige adipocyte population regardless of cold stimulation, whereas removing Hdac4 in Lkb1^{AKO} mice restored responsiveness to cold (Fig. 5*D*), suggesting that Hdac4 activation in adipocytes determines dynamic behavior of beige adipocytes. Further studies are warranted to investigate how beige adipocytes reprogram during their transitions (beige to white and to beige again by cold) and what are the Hdac4-dependent and white adipocyte–derived signals that maintain characteristics of preexisting beige adipocytes in iWAT.

Classic brown adipocytes and beige adipocytes are capable of Ucp1-dependent thermogenesis. The classic brown adipocytes may be the major heat-producing Ucp1^{+} adipocytes in the setting of hypothermia. In our Ucp1-Cre;Rosa-iDTR mice, iBAT regeneration occurred rapidly after DT-mediated ablation of all Ucp1^{+} brown and beige adipocytes. The regenerated iBAT itself sufficiently rendered cold resistance regardless of beige adipocyte numbers. However, beige adipocytes could contribute to thermogenesis significantly in the absence of functional iBAT. Mice lacking Bmpr1a in Myf5^{+} lineage cells exhibited iBAT defect and compensatory increase in beige adipocytes (47). However, a compensatory increase of sympathetic inputs to iWAT at room temperature was not observed in Lkb1^{AKO} mice. One of possible explanations is that metabolic reprogramming in mitochondria caused by Lkb1 deficiency (48) might be sufficient to cope with mild cold stress (room-temperature housing), but not with strong cold stress (4°C cold-tolerance test).

Improved metabolic performance accompanied by beige adipocyte expansion was also observed in Ucp1 KO mice

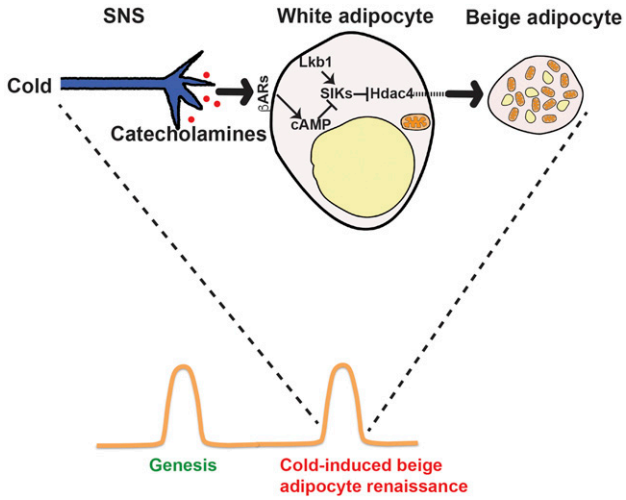

Figure 8—Diagram showing cellular and molecular mechanisms of cold-induced beige adipocyte renaissance. Under cold stimulation, adipocyte Hdac4 activation could promote beige adipocyte renaissance noncell autonomously. Lkb1 activates SIKs to suppress Hdac4 activation, whereas cold stimulates Hdac4 activation through βAR-mediated inhibition of SIKs. Additional mechanisms of cold-induced beige adipocyte de novo formation demonstrated in other studies not shown in this image.

alone or together with the inactivation of the glycerol phosphate cycle (49,50); however, it has not been demonstrated whether expanded beige adipocytes did functionally contribute to their elevated energy expenditure and/or decreased adiposity under HFD in vivo. Our studies suggest that thermogenic capacity and metabolic homeostasis are uncoupled in Lkb1^{AKO} mice. For example, mice with Ucp1-Cre–mediated deletion of Lkb1 specifically in brown and beige adipocytes, the Lkb1^{BKO} mice, showed similar metabolic improvements under HFD without beige adipocyte expansion. This suggests that Lkb1 deficiency in iBAT alone may improve metabolic performances in Lkb1^{AKO} mice, although we cannot absolutely rule out possible contributions of Lkb1 deletion in other adipose depots. Beige adipocyte expansion is dependent on Hdac4 activation in white adipocytes. Removing Hdac4 demolishes beige adipocyte population in iWAT of Lkb1^{AKO} mice in adult mice without thermogenic or metabolic consequences. Therefore, beige adipocytes do not contribute to metabolic benefits observed in Lkb1^{AKO} mice. However, beige adipocytes may influence energy homeostasis through thermogenic and nonthermogenic functions in other settings. Because Lkb1 regulates the SIK-Hdac4 pathway specifically in white adipocytes to promote beige adipocyte renaissance in adult mice, additional animal models that only target the Lkb1-dependent beige adipocyte renaissance program and spontaneously preserve iBAT thermogenesis may reveal specific functions of beige adipocytes and novel therapeutic approaches to tackle metabolic disorders.

Acknowledgments. The authors thank C. Paillart at the University of California, San Francisco Diabetes Center for assistance in CLAMS experiments, R. Lao at the University of California, San Francisco Next Generation Sequencing Core for RNA-seq, and A. Williams at the Gladstone Bioinformatics Core for assistance with statistical analysis of sequence data. The authors also thank Drs. E. Olson (University of Texas Southwestern), E. Rosen (Harvard University), and H. Takemori (National Institute of Biomedical Innovation) for floxed Hdac4, Ucp1-Cre, and Sik2-null mice, respectively, and the Knockout Mouse Project for Sik1-null mice.

Funding. This work was supported by National Institutes of Health grants P30-DK-063720 (to University of California, San Francisco Diabetes Center) and P30-DK-098722 (to University of California, San Francisco Nutrition Obesity Research Center), research grants from the Larry L. Hillblom Foundation and JDRF (to B.W.), and National Institutes of Health grants R01 DK-105175 (to B.W.), CA-139158 (to W.H.), DK-094641 (to A.C.), and DK-101064 (to A.C.). E.P. is supported by a fellowship grant from the Larry L. Hillblom Foundation. Y. Wu is supported by an Agency for Science, Technology and Research fellowship.

Duality of Interest. No potential conflicts of interest relevant to this article were reported.

Author Contributions. Y.Wa., E.P., and B.W. planned the experiments and wrote the paper. Y.Wa. and E.P. performed most of the experiments. D.W. performed initial characterization of SIK-deficient mice. W.H. assisted with Ucp1 staining in adipose tissue. Y. Wu and A.C. analyzed Pdgfra^{+}Sca1^{+} progenitors in adipose tissues. B.W. is the guarantor of this work and, as such, had full access to all of the data in the study and takes responsibility for the integrity of the data and the accuracy of the data analysis.

Prior Presentation. Parts of this study were presented in abstract form at the 76th Scientific Sessions of the American Diabetes Association, New Orleans, LA, 10–14 June 2016.

References

1. Spiegelman BM, Flier JS. Obesity and the regulation of energy balance. Cell 2001;104:531–543
2. Cannon B, Nedergaard J. Brown adipose tissue: function and physiological significance. Physiol Rev 2004;84:277–359
3. Golozoubova V, Cannon B, Nedergaard J. UCP1 is essential for adaptive adrenergic nonshivering thermogenesis. Am J Physiol Endocrinol Metab 2006;291:E350–E357
4. Shabalina IG, Petrovic N, de Jong JM, Kalinovich AV, Cannon B, Nedergaard J. UCP1 in brite/beige adipose tissue mitochondria is functionally thermogenic. Cell Reports 2013;5:1196–1203
5. Cypess AM, Lehman S, Williams G, et al., Identification and importance of brown adipose tissue in adult humans. N Engl J Med 2009;360:1509–1517
6. van Marken Lichtenbelt WD, Vanhommerig JW, Smulders NM, et al. Cold-activated brown adipose tissue in healthy men. N Engl J Med 2009;360:1500–1508
7. Virtanen KA, Lidell ME, Orava J, et al. Functional brown adipose tissue in healthy adults. N Engl J Med 2009;360:1518–1525
8. Seale P, Bjork B, Yang W, et al. PRDM16 controls a brown fat/skeletal muscle switch. Nature 2008;454:961–967
9. Barbatelli G, Murano I, Madsen L, et al. The emergence of cold-induced brown adipocytes in mouse white fat depots is determined predominantly by white to brown adipocyte transdifferentiation. Am J Physiol Endocrinol Metab 2010;298:E1244–E1253
10. Cousin B, Cinti S, Morroni M, et al. Occurrence of brown adipocytes in rat white adipose tissue: molecular and morphological characterization. J Cell Sci 1992;103:931–942
11. Granneman JG, Li P, Zhu Z, Lu Y. Metabolic and cellular plasticity in white adipose tissue I: effects of beta3-adrenergic receptor activation. Am J Physiol Endocrinol Metab 2005;289:E608–E616
12. Himms-Hagen J, Melnyk A, Zingaretti MC, Ceresi E, Barbatelli G, Cinti S. Multilocular fat cells in WAT of CL-316243-treated rats derive directly from white adipocytes. Am J Physiol Cell Physiol 2000;279:C670–C681

13. Jimenez M, Barbatelli G, Allevi R, et al. Beta 3-adrenoceptor knockout in C57BL/6J mice depresses the occurrence of brown adipocytes in white fat. Eur J Biochem 2003;270:699–705
14. Altshuler-Keylin S, Shinoda K, Hasegawa Y, et al. Beige adipocyte maintenance is regulated by autophagy-induced mitochondrial clearance. Cell Metab 2016;24: 402–419
15. Wang H, Liu L, Lin JZ, Aprahamian TR, Farmer SR. Browning of white adipose tissue with roscovitine induces a distinct population of UCP1(+) adipocytes. Cell Metab 2016;24:835–847
16. Nedergaard J, Cannon B. The browning of white adipose tissue: some burning issues. Cell Metab 2014;20:396–407
17. Nguyen KD, et al. Alternatively activated macrophages produce catecholamines to sustain adaptive thermogenesis. Nature 2011;480:104–108
18. Cheng W, Zhu Z, Jin X, Chen L, Zhuang H, Li F. Intense FDG activity in the brown adipose tissue in omental and mesenteric regions in a patient with malignant pheochromocytoma. Clin Nucl Med 2012;37:514–515
19. Soloveva V, Graves RA, Rasenick MM, Spiegelman BM, Ross SR. Transgenic mice overexpressing the beta 1-adrenergic receptor in adipose tissue are resistant to obesity. Mol Endocrinol 1997;11:27–38
20. Wu J, Cohen P, Spiegelman BM. Adaptive thermogenesis in adipocytes: is beige the new brown? Genes Dev 2013;27:234–250
21. Harms M, Seale P. Brown and beige fat: development, function and therapeutic potential. Nat Med 2013;19:1252–1263
22. Kozak LP. The genetics of brown adipocyte induction in white fat depots. Front Endocrinol (Lausanne) 2011;2:64
23. Rosenwald M, Perdikari A, Rülicke T, Wolfrum C. Bi-directional interconversion of brite and white adipocytes. Nat Cell Biol 2013;15:659–667
24. Lee YH, Petkova AP, Konkar AA, Granneman JG. Cellular origins of cold-induced brown adipocytes in adult mice. FASEB J 2015;29:286–299
25. Mihaylova MM, Vasquez DS, Ravnskjaer K, et al Class IIa histone deacetylases are hormone-activated regulators of FOXO and mammalian glucose homeostasis. Cell 2011;145:607–621
26. Wang B, Moya N, Niessen S, et al A hormone-dependent module regulating energy balance. Cell 2011;145:596–606
27. Choi S, Lim DS, Chung J. Feeding and fasting signals converge on the LKB1-SIK3 pathway to regulate lipid metabolism in Drosophila. PLoS Genet 2015;11: e1005263
28. Contreras GA, Lee YH, Mottillo EP, Granneman JG. Inducible brown adipocytes in subcutaneous inguinal white fat: the role of continuous sympathetic stimulation. Am J Physiol Endocrinol Metab 2014;307:E793–E799
29. Chabowska-Kita A, et al Low ambient temperature during early postnatal development fails to cause a permanent induction of brown adipocytes. FASEB J 2015; 29:3238–3252
30. Kozak LP, Koza RA, Anunciado-Koza R, Mendoza T, Newman S. Inherent plasticity of brown adipogenesis in white fat of mice allows for recovery from effects of post-natal malnutrition. PLoS One 2012;7:e30392
31. Lee YH, Petkova AP, Mottillo EP, Granneman JG. In vivo identification of bipotential adipocyte progenitors recruited by β3-adrenoceptor activation and high-fat feeding. Cell Metab 2012;15:480–491
32. Buch T, Heppner FL, Tertilt C, et al. A Cre-inducible diphtheria toxin receptor mediates cell lineage ablation after toxin administration. Nat Methods 2005;2:419–426
33. Vishvanath L, et al. Pdgfrβ+ mural preadipocytes contribute to adipocyte hyperplasia induced by high-fat-diet feeding and prolonged cold exposure in adult mice. Cell Metab 2016;23:350–359
34. Wang QA, Tao C, Gupta RK, Scherer PE. Tracking adipogenesis during white adipose tissue development, expansion and regeneration. Nat Med 2013;19:1338–1344
35. Berry DC, Jiang Y, Graff JM. Mouse strains to study cold-inducible beige progenitors and beige adipocyte formation and function. Nat Commun 2016;7:10184
36. Lee YH, Petkova AP, Granneman JG. Identification of an adipogenic niche for adipose tissue remodeling and restoration. Cell Metab 2013;18:355–367
37. Wang B, Goode J, Best J, et al. The insulin-regulated CREB coactivator TORC promotes stress resistance in Drosophila. Cell Metab 2008;7:434–444
38. Screaton RA, Conkright MD, Katoh Y, et al. The CREB coactivator TORC2 functions as a calcium- and cAMP-sensitive coincidence detector. Cell 2004;119:61–74
39. Berdeaux R, Goebel N, Banaszynski L, et al. SIK1 is a class II HDAC kinase that promotes survival of skeletal myocytes. Nat Med 2007;13:597–603
40. Park J, Yoon YS, Han HS, et al. SIK2 is critical in the regulation of lipid homeostasis and adipogenesis in vivo. Diabetes 2014;63:3659–3673
41. Muraoka M, Fukushima A, Viengchareun S, et al. Involvement of SIK2/TORC2 signaling cascade in the regulation of insulin-induced PGC-1alpha and UCP-1 gene expression in brown adipocytes. Am J Physiol Endocrinol Metab 2009;296:E1430–E1439
42. Mottillo EP, Desjardins EM, Crane JD, et al. Lack of adipocyte AMPK exacerbates insulin resistance and hepatic steatosis through brown and beige adipose tissue function. Cell Metab 2016;24:118–129
43. Shan T, Xiong Y, Zhang P, et al. Lkb1 controls brown adipose tissue growth and thermogenesis by regulating the intracellular localization of CRTC3. Nat Commun 2016;7:12205
44. Butler AA, Kozak LP. A recurring problem with the analysis of energy expenditure in genetic models expressing lean and obese phenotypes. Diabetes 2010;59: 323–329
45. Tschöp MH, Speakman JR, Arch JR, et al. A guide to analysis of mouse energy metabolism. Nat Methods 2011;9:57–63
46. Long JZ, Svensson KJ, Tsai L, et al. A smooth muscle-like origin for beige adipocytes. Cell Metab 2014;19:810–820
47. Schulz TJ, Huang P, Huang TL, et al. Brown-fat paucity due to impaired BMP signalling induces compensatory browning of white fat. Nature 2013;495:379–383
48. Faubert B, Vincent EE, Griss T, et al. Loss of the tumor suppressor LKB1 promotes metabolic reprogramming of cancer cells via HIF-1α. Proc Natl Acad Sci U S A 2014;111:2554–2559
49. Liu X, Rossmeisl M, McClaine J, Riachi M, Harper ME, Kozak LP. Paradoxical resistance to diet-induced obesity in UCP1-deficient mice. J Clin Invest 2003;111: 399–407
50. Anunciado-Koza R, Ukropec J, Koza RA, Kozak LP. Inactivation of UCP1 and the glycerol phosphate cycle synergistically increases energy expenditure to resist diet-induced obesity. J Biol Chem 2008;283:27688–27697